machines

MDPI

Article

Minimization Method for 3D Surface Roughness Evaluation Area

Viktor Molnár

Institute of Manufacturing Science, University of Miskolc, H-3515 Miskolc, Hungary; viktor.molnar@uni-miskolc.hu

Abstract: 3D surface roughness measurement is still a less mature procedure than its 2D version. The size of the evaluation area is not as standardized as the measurement length in the 2D version. The purpose of this study is to introduce a method for minimizing the evaluated surface area. This could help industrial applications in minimizing the time and cost of measurements. Machining experiments (hard turning and infeed grinding) and surface roughness measurements were carried out for automotive industrial parts to demonstrate the introduced method. Some frequently used roughness parameters were analyzed. Basic statistical calculations were applied to analyze the relationship between the surface area and the roughness parameter values and regression analyses were applied to validate the results in case of the applied technological data. The main finding of the study is that minimum evaluation areas can be clearly designated and, depending on the different roughness parameter–procedure version, different evaluation sizes (Sa: 1.3 × 1.3 mm; Sq: 1.4 × 1.4 mm; Ssk and Sku: 2 × 2 m; Sp and Sv: 1.7 × 1.7 mm) are recommended.

Keywords: 3D surface roughness; hard turning; grinding

Citation: Molnár, V. Minimization Method for 3D Surface Roughness Evaluation Area. *Machines* **2021**, *9*, 192. https://doi.org/10.3390/machines9090192

Academic Editor: Gianni Campatelli

Received: 6 August 2021
Accepted: 4 September 2021
Published: 8 September 2021

1. Introduction

Surface roughness of machined surfaces has a high impact on the working characteristics [1,2] and wear and therefore on the lifetime of the components built into automotive industrial products. In cutting, the final surface topography depends on the tool and workpiece material pair, the tool geometry and the kinematic characteristics of the machining procedure. This effect can clearly be observed by studying theoretical roughness parameter values in machining by fixed [3] or rotational tools [4,5]. Therefore, planning the machining conditions and data requires special attention, particularly in finishing operations. Today in precision machining it is not enough anymore to ensure a specific value of a certain surface roughness parameter; instead, complex analysis of the surface topography is essential. If, for example, the purpose is increasing the tool life in machining hardened surfaces, a decision must be made among the hard machining procedures (machining by single-point or abrasive tool). If a specified roughness value can be realized by not only grinding but—e.g., by hard turning too—after the appropriate determination of the cutting data, a more profound analysis is necessary to make the decision [6]. The deep analysis of surface textures can act as a potential predictor of machining performance [7,8].

During the last decades, many scientists and constructors became convinced that the third dimension should be added to the surface analysis. At present, 3D analysis of the surface geometry is widely accepted [9]. Characterization of surface texture is essential, particularly in high-tech applications [10] and 3D roughness parameters are more suitable for this purpose than the 2D ones [11]. Surface texture metrology gives a better understanding of the surface in its functional state [12]. In hard turning the 3D parameters are useful in more detailed analyses of certain characteristic features of the machined surface [13–15]. This can be stated for grinding too [16,17]. However, this is hardly generalizable for the hard machining procedures, as the results are obtained mostly for a single material and the cutting parameters are in a narrow range. Most

of the studies analyze only a single or a few roughness parameters or the topography diagram without analyzing a set of parameters in a complex manner. There are, however, experimental studies with well-founded design serve as the basis of complex analyses and can provide information about the sensitivity of the cutting data on the roughness parameter values [18,19].

Several studies have recently been published in which 3D surface roughness measurement was the focus of the analysis. It has been applied for various machining procedures such as hard turning [20], turning [21], abrasive waterjet cutting (AWC) [22,23], diamond turning [24], shot peening [18], micro milling [25], selective laser melting (SLM) [19,26], or electrical discharge machining (EDM) [27]. There are studies that focus on the effect of process parameters [18,19] or cutting data [21,25] on the surface roughness. At the same time, 3D roughness parameters or studies can be applicable for wear prediction [12] or cutting insert selection [28], or in analyzing surface erosion processes [10].

In this paper, the bore surfaces of gears built into transmission systems are analyzed. Due to the wide use of gears, research studies must focus on these basic automotive industrial components. The reason for this is not only scientific interest, but also a need by the industry [29]. "The gear industry is a multi-million industry with a constant annual increase in turnover that is projected to be worth over USD 210 billion in 2026. In order to achieve the production rates needed, the use of efficient manufacturing processes is crucial" [30].

The problem that led to this study was that several 3D topography research studies are available but there is no exact advice for the evaluation area of the surface in them, nor in the relevant standards. It is important to carry out experiments that focus on the minimum size of the measured area. This could influence the values of surface roughness parameters [9]. A survey of several studies revealed that the evaluation area seems to vary in a random manner, i.e., no relationship can be observed between the evaluation area and the applied machining procedure. Studies with the focus of minimization of the evaluation area can hardly be found [31]. In Table A1, examples are collected to demonstrate this phenomenon. In quite many studies important information is neglected, which means that the experiment cannot be replicated. Such problems are for example no information on evaluation area [32,33], the cut-off or filtering method [34,35], or all of these [36,37].

The purpose of this study is the reduction of measurement and therefore the evaluation area in 3D roughness measurement. Parameters for height (Sa, Sq, Ssk, Sku, Sp, and Sv) are measured and analyzed in different evaluation areas (from 2 × 2 mm to 0.2 × 0.2 mm) and minimum areas were aimed to be determined by applying regression analysis and basic statistical calculations.

For the minimization of the evaluation area first the changes in the analyzed roughness values and their standard deviations were studied when reducing the evaluation area. This step resulted in the observation that distortion in the roughness data occurs to some extent. In the second step, the minimum evaluation areas were determined for each roughness parameter based on the designated difference limit in the roughness data when the evaluation area is decreased and on a designated standard deviation limit. In the third step, regression analyses were carried out to validate the determined minimum areas based on the deviation resulting from the randomness of the roughness data. In surface roughness analysis this method is not unique. Kluz et al. applied it for testing the characteristics of 2D roughness parameters [38]. In the present study, the minimization is not generalizable, the results can be considered as those of a case study; they are valid only for the analyzed procedure versions and technological parameters. The novelty lies in the method of the minimization, which can be applied to a wider range of technological parameters and machining procedures. The minimization method was tested by concrete cutting experiments; therefore, the results can contribute to further studies.

2. Experimental and Measurement Setup

In the experiment, internal cylindrical surfaces of gear wheels were machined. The material of the workpieces was 20MnCr5; its physical and mechanical properties and chemical composition are summarized in Tables 1 and 2.

Table 1. Physical and mechanical properties of 20MnCr5.

Yield Strength σ_s (MPa)	Tensile Strength σ_b (MPa)	Hardness HRC	Thermal Conductivity k (W/mK)	Density ρ (g/cm^3)	Elastic Modulus E (GPa)
1034	1158	62–64	11.7	7.7–8.03	190–210

Table 2. Chemical composition of 20MnCr5.

C	Si	Mp	S	P	Cr	Cu	Al
0.17–0.22	≤0.4	1.1–1.4	≤0.035	≤0.025	1.0–1.3	≤0.4	0.02–0.04

The bore lengths of the workpieces were L = 34 mm and their diameters were d = 88 mm. The bores were machined in the experiments on the whole bore length (L) Two workpieces were machined by hard turning and one by infeed grinding. Both the hard turning and the grinding were carried out on a hard turning lathe type EMAG VSC 400 (Figure 1a,b). The following tools were applied in the experiments:

- Turning insert: Sandvik CCGW 09T308 NC2
- Tool holder: E25T-SCLCR 09-R
- Grinding wheel: Norton 3AS80J8VET 01_36X37X13

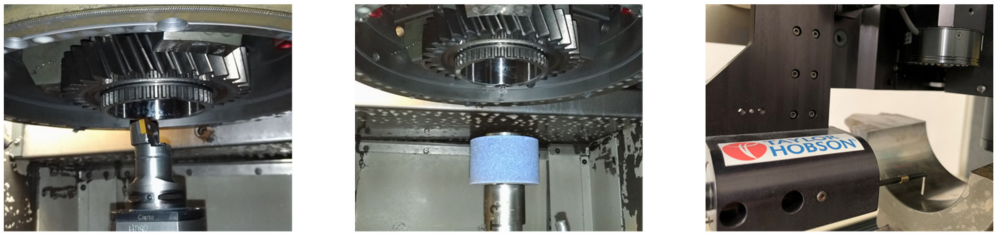

(**a**) (**b**) (**c**)

Figure 1. Machining and measurement setup of the workpiece: (**a**) hard turning, (**b**) infeed grinding, (**c**) measurement by inductive sensor.

Three procedure versions were applied in the experiments: M1 and M2 were hard turning with different feeds and M3 was infeed grinding. The cutting parameters were within the limits recommended by the tool manufacturer. The technological data of the hard turning procedure versions:

- Feed: f = 0.1 mm/rev (M1); f = 0.3 mm/rev (M2)
- Depth-of-cut: a_p = 0.2 mm
- Workpiece rpm: n = 615 min^{-1}

The technological data of the grinding procedure version:

- Feed: f = 0.01 mm/rev
- Wheel width: L' = 36 mm
- Infeed depth (radial allowance): Δ = 0.2 mm
- Workpiece rpm: n_w = 325 min^{-1}
- Tool rpm: n_t = 20,000 min^{-1}

The 3D surface roughness measurements were carried out by the measuring machine AltiSurf 520 (Figure 1c). The applied sensor was a contact type inductive sensor, the radius

of the stylus was 2 µm. The nominal measurement range was 150–1500 µm, the resolution in Z direction was 1 µm and in X and Y direction 2 µm. The standard applied for the evaluation was ISO 25178-2:2012. The scanned area was 2.8 × 2.8 mm and the evaluation area was 2 × 2 mm (the cut-off was 0.8 mm and Gauss filter was applied). The number of scanned points per measurement was 1 million. The different evaluation area sizes were designated by the data processing software of the measuring machine (Altimap Premium). One area was scanned on each workpiece. A total of 19 areas of different sizes were evaluated. The scheme of this is demonstrated in Figure 2.

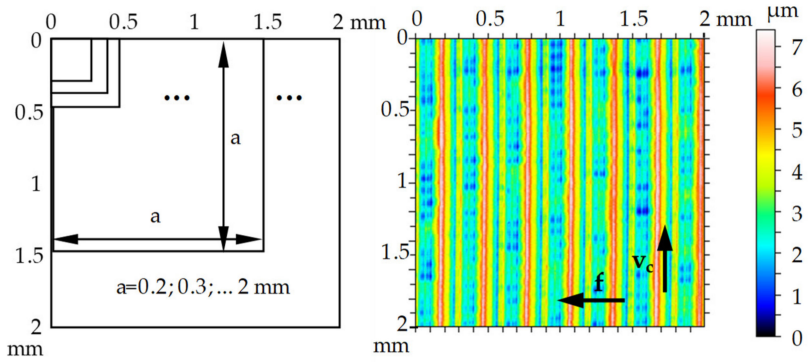

Figure 2. Area sizes applied in the regression analyses.

The analyzed roughness parameters and their calculations (Equations (1)–(6)):

- Arithmetical mean height (Sa, µm): A relatively frequent roughness parameter in part drawings.

$$\mathrm{Sa} = \frac{1}{\mathrm{A}} \iint_{\mathrm{A}} |Z(x,\, y)| dxdy \tag{1}$$

- Root mean square height (Sq, µm): It can be used to qualify the topography of relatively smooth surfaces. It is sensitive to the outlier surface peaks and valleys.

$$\mathrm{Sq} = \sqrt{\frac{1}{\mathrm{A}} \iint_{\mathrm{A}} Z^2(x,\, y) dxdy} \tag{2}$$

- Skewness (Ssk, –): The working surfaces are characterized by the skewness; it characterizes the tribological properties of the surface. A positive value means the dominance of roughness peaks and a negative value means the dominance of valleys and usually better lubrication.

$$\mathrm{Ssk} = \frac{1}{\mathrm{Sq}^3} \left[\frac{1}{\mathrm{A}} \iint_{\mathrm{A}} Z^3(x,\, y) dxdy \right] \tag{3}$$

- Kurtosis (Sku, –): It characterizes the tribological properties. It is generally considered together with Ssk. It informs about the lubrication and wear resistance.

$$\mathrm{Sku} = \frac{1}{\mathrm{Sq}^4} \left[\frac{1}{\mathrm{A}} \iint_{\mathrm{A}} Z^4(x,\, y) dxdy \right] \tag{4}$$

- Maximum peak height (Sp, µm): It is the height of the highest peak within the evaluation area.

$$\mathrm{Sp} = \max_{\mathrm{A}} z(x,\, y) \tag{5}$$

- Maximum pit height (Sv, μm): It is the absolute value of the height of the largest pit within the evaluated area.

$$\mathrm{Sv} = \left| \min_{\mathrm{A}} z(x, y) \right| \tag{6}$$

3. Results and Discussion

The measured values of the roughness parameters are summarized in Appendix B (Tables A2–A4). The 3D topography pictures are collected in Appendix C (Figure A1). In Section 3.1, some observations are made based on the measured and calculated data and in the proceeding sections the minimization of the evaluation area is described. In Figure 3, the minimization process is drafted.

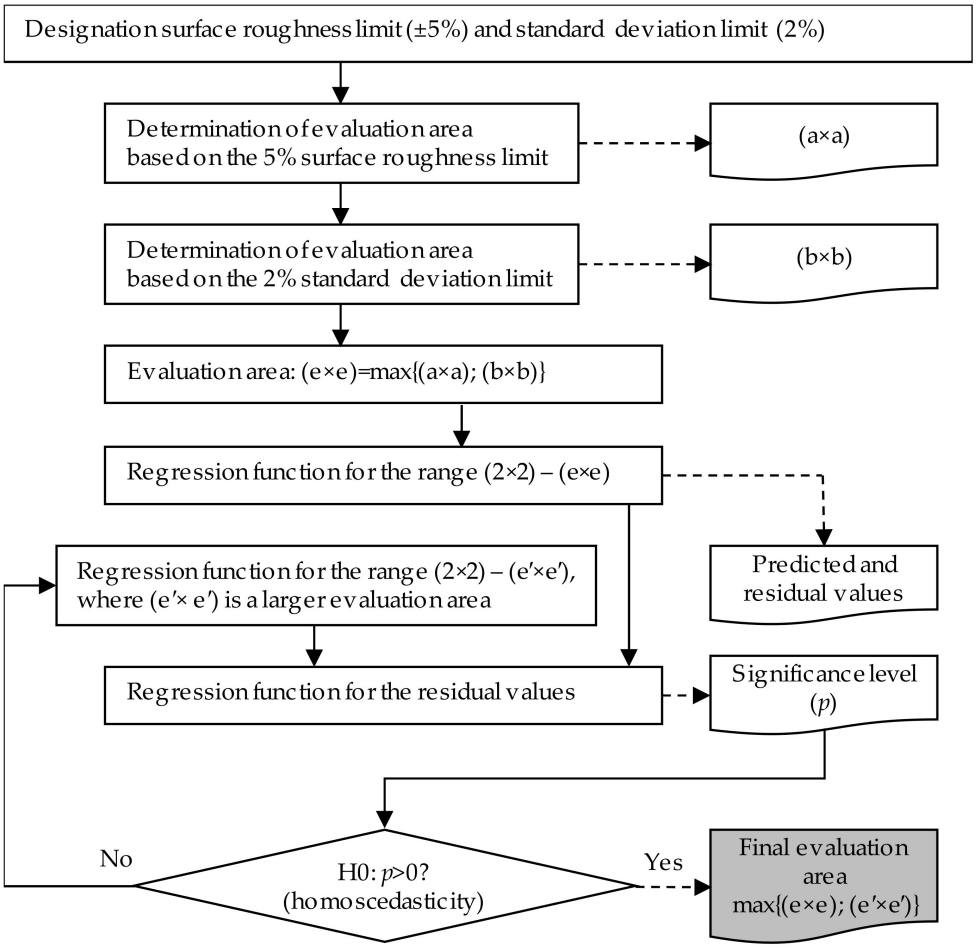

Figure 3. Process of the minimization of the evaluation area.

3.1. The Surface Roughness Values and Their Standard Deviations

With the decrease of the evaluation area the roughness values become distorted. To get familiar with this phenomenon, it is useful to analyze the absolute values of the roughness parameters and their standard deviations. The surface roughness measurement results and their standard deviations were plotted in Figures 4–9. The first value of the standard deviation was calculated for the first three (2 × 2 mm–1.8 × 1.8 mm) and the further values for four, five, etc. roughness data. To facilitate the comparison of the procedure versions in the case of a given roughness parameter, the maximum values of the axes (roughness and standard deviation) were set to identical values for the three procedure versions.

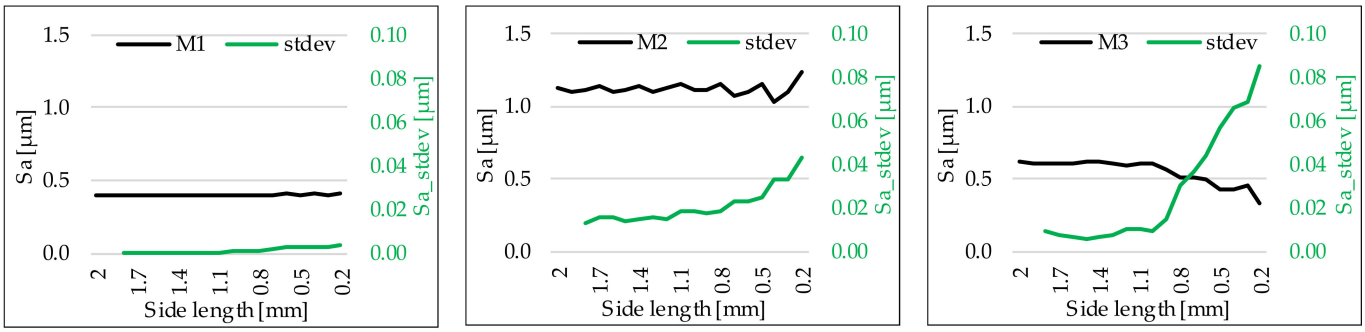

(**a**) (**b**) (**c**)

Figure 4. Sa parameters (black) and their standard deviations (green) as a function of the analyzed area (2 × 2 mm–0.2 × 0.2 mm): (**a**) M1—hard turning, f = 0.1 mm/rev; (**b**) M2—hard turning, f = 0.3 mm/rev; (**c**) M3—grinding.

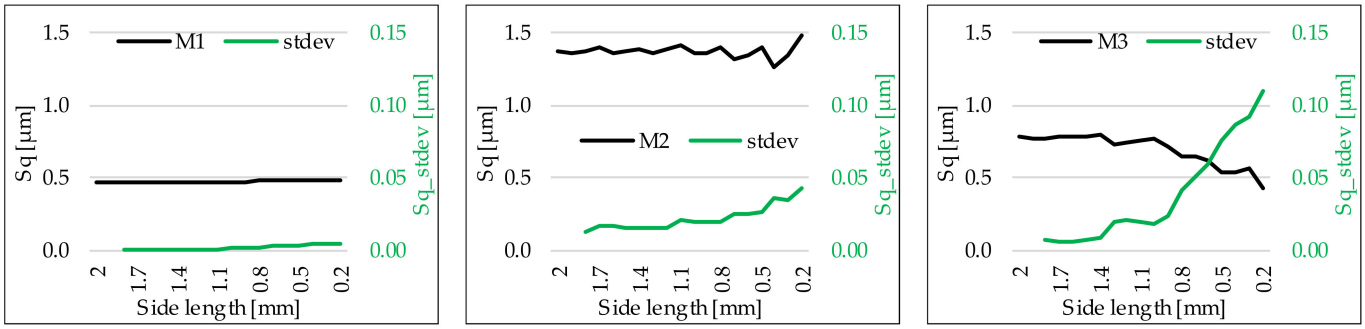

(**a**) (**b**) (**c**)

Figure 5. Sq parameters (black) and their standard deviations (green) as a function of the analyzed area (2 × 2 mm–0.2 × 0.2 mm): (**a**) M1—hard turning, f = 0.1 mm/rev; (**b**) M2—hard turning, f = 0.3 mm/rev; (**c**) M3—grinding.

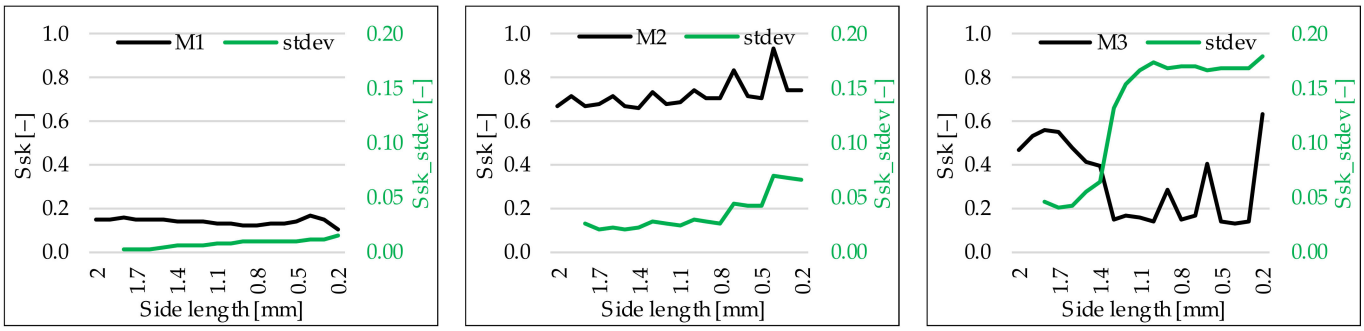

(**a**) (**b**) (**c**)

Figure 6. Ssk parameters (black) and their standard deviations (green) as a function of the analyzed area (2 × 2 mm–0.2 × 0.2 mm): (**a**) M1—hard turning, f = 0.1 mm/rev; (**b**) M2—hard turning, f = 0.3 mm/rev; (**c**) M3—grinding.

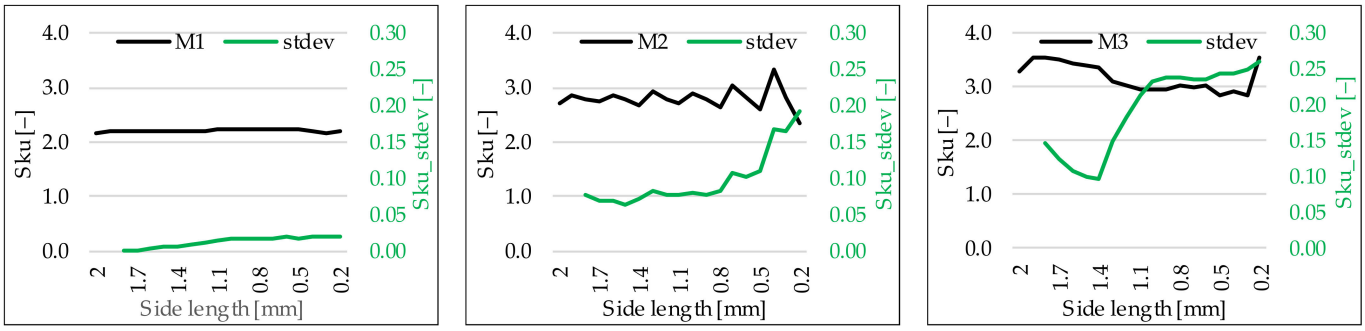

(**a**) (**b**) (**c**)

Figure 7. Sku parameters (black) and their standard deviations (green) as a function of the analyzed area (2 × 2 mm–0.2 × 0.2 mm): (**a**) M1—hard turning, f = 0.1 mm/rev; (**b**) M2—hard turning, f = 0.3 mm/rev; (**c**) M3—grinding.

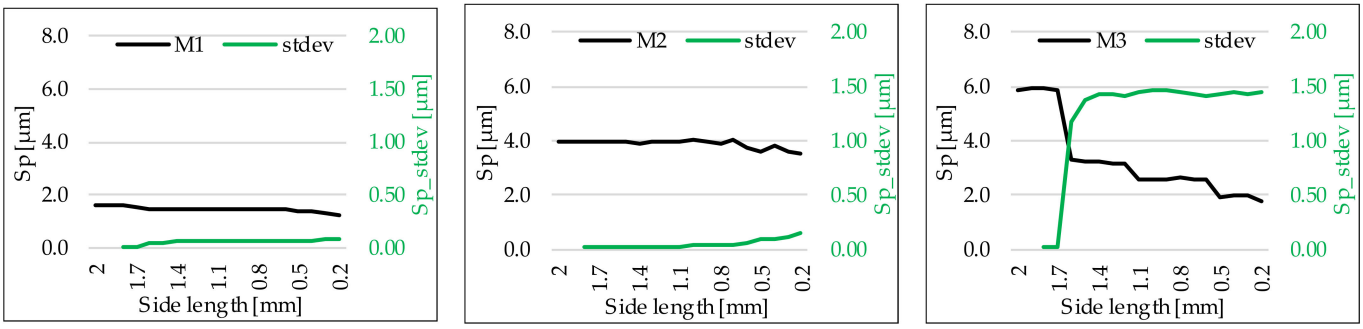

(**a**) (**b**) (**c**)

Figure 8. Sp parameters (black) and their standard deviations (green) as a function of the analyzed area (2 × 2 mm–0.2 × 0.2 mm): (**a**) M1—hard turning, f = 0.1 mm/rev; (**b**) M2—hard turning, f = 0.3 mm/rev; (**c**) M3—grinding.

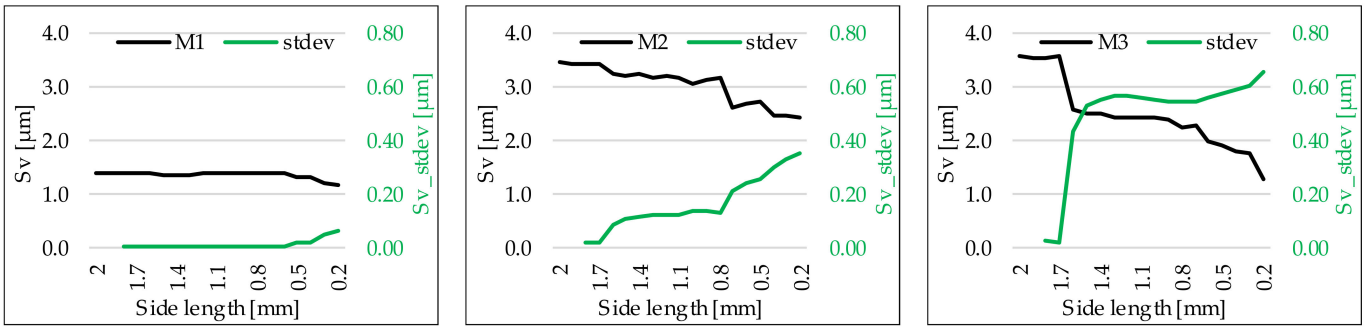

(**a**) (**b**) (**c**)

Figure 9. Sv parameters (black) and their standard deviations (green) as a function of the analyzed area (2 × 2 mm–0.2 × 0.2 mm): (**a**) M1—hard turning, f = 0.1 mm/rev; (**b**) M2—hard turning, f = 0.3 mm/rev; (**c**) M3—grinding.

It has to be noted that some of the roughness values of the ground surface were higher than those of the surface turned by f = 0.1 mm/rev feed. The reason for this is that the feed value is significantly low compared to the radius of the insert (0.8 mm). Therefore, the burnishing effect is determinant. When increasing the feed to 0.3 mm/rev, the imprint of the insert become determinant in the topography.

The initial assumption was that the distortion of the surface roughness values (plotted black curves) would increase with the decrease of the measured area.

In the case of the Sa—M2 roughness parameter—procedure version pair (Figure 4b) it can be observed that with the decrease of the measured area an intense oscillation occurs in the roughness value (on both sides of the average). Concerning the Sa—M3 pair

(Figure 4c), a slight decrease in the roughness value can be observed with a fluctuation in the background:

Concerning the Sq—M2 and the Sq—M3 pairs (Figure 5b,c), the same can be observed as in the cases of the Sa—M2 and Sa—M3 pairs.

Concerning the Ssk—M2 and the Sku—M2 (Figures 6b and 7b) roughness parameter—procedure version pairs, intense oscillations occur in the roughness values. The roughness values of the surface hard turned by f = 0.1 mm/rev show only a negligible deviation (Figures 6a and 7a) and there is no trend or periodicity in the roughness data of the ground surface (Figures 6c and 7c).

Concerning the Sp—M1, Sp—M2 (Figure 8a,b), the Sv—M1 and Sv—M2 (Figure 9a,b) pairs slight decreases can be observed with a fluctuation in the background. The maximum peak height (Sp) and maximum pit height (Sv) are relatively sensitive to outliers, and significant 'jumps' can be observed in the roughness parameter values: Sp—M3 (Figure 8c) and Sv—M3 (Figure 9c). Here first the outlying surface points were within the evaluated area (Figure 10) and when the measured area decreased to 1.6 × 1.6 mm, the outliers disappeared and the Sp and Sv values started to show slight decreases.

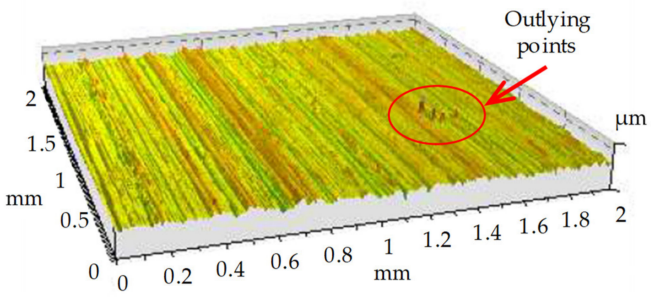

Figure 10. Outliers on the ground surface (procedure version M3).

Because of these observations, the standard deviations of the data were calculated and plotted. In the most cases the deviation increased with the decrease of the measured area, e.g., Sa–M2 (Figure 4b); Sku–M2 (Figure 7b); Sp–M1 (Figure 8a). When there were sudden changes in the parameter values, they showed up in the deviation values too. For example, a clear decrease can be observed in the first five deviation values of the roughness parameter—procedure version pair Sku–M3 (Figure 7c).

The observations connected to the roughness diagrams and standard deviation diagrams clearly show that there are deviations in the roughness values. However, more detailed quantification of the deviation is necessary.

3.2. Designation of Minimum Evaluation Areas

With the decrease of the evaluation area, a trend or an oscillation or both can be observed in the roughness curves. There is a difference between the roughness value of the 2 × 2 mm area and that of a smaller area. Let the maximum limit of the absolute value of this difference be 5%. This extent in this study and in industrial practice is considered as a negligible error. Concerning the standard deviation values, a similar limit can be designated. 2% of the roughness value measured on the 2 × 2 mm area (2%_$S_{2\times2}$) is statistically low enough to serve as a limit for the standard deviation. With the decrease of the evaluation area the standard deviation increases. Another minimum evaluation area is where the standard deviation does not exceed the 2% limit. This different point of view helps in refining the minimum areas designated by the 5% limit of the absolute roughness values. The two methods are demonstrated in Figure 11.

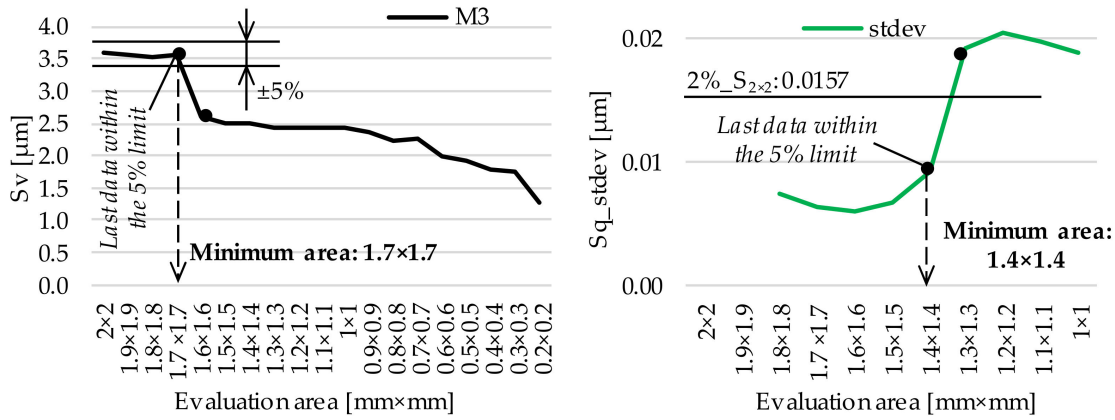

(**a**) (**b**)

Figure 11. Schemes of designation minimum evaluation areas with limits set based on (**a**) roughness values and their (**b**) standard deviations.

The absolute differences are collected in Table 3. The minimum evaluation area is where this limit is not reached when the values from the 2 × 2 mm area to the direction of the smaller ones are considered. In Table 3 the first differences which do not exceed the limit are underlined. The minimum areas gained by this approach is considered as the first step of the minimization.

Table 3. Changes in the roughness values (%) compared to the values measured on the area 2 × 2 mm.

		Side Length of the Measured Area (Square) (mm)																		
		2.0	**1.9**	**1.8**	**1.7**	**1.6**	**1.5**	**1.4**	**1.3**	**1.2**	**1.1**	**1.0**	**0.9**	**0.8**	**0.7**	**0.6**	**0.5**	**0.4**	**0.3**	**0.2**
Sa (µm)	M1	0.0	0.1	0.1	0.2	0.2	0.1	0.0	0.1	0.1	0.0	0.3	0.5	0.9	1.5	1.9	1.3	2.0	1.4	2.0
	M2	0.0	2.2	0.8	1.1	2.0	1.2	1.0	2.2	0.0	2.8	1.9	1.6	2.0	5.1	2.9	2.8	9.2	3.0	10
	M3	0.0	2.9	2.2	1.6	1.6	1.0	0.1	3.4	5.2	3.0	2.6	8.9	18	18	21	31	31	27	46
Sq (µm)	M1	0.0	0.0	0.1	0.2	0.1	0.0	0.1	0.3	0.4	0.4	0.7	0.9	1.4	1.9	2.2	1.4	2.1	1.1	2.1
	M2	0.0	1.8	0.4	1.3	1.6	0.9	0.8	1.7	0.3	2.8	1.5	1.1	1.7	4.5	2.3	2.0	7.9	2.5	7.0
	M3	0.0	1.9	1.0	0.6	0.2	0.5	1.8	6.4	4.7	3.0	2.3	8.8	18	18	21	31	32	28	45
Ssk (–)	M1	0.0	2.0	0.7	1.5	4.6	5.6	9.0	11	9.3	14	13	18	20	16	16	10	10	4.8	32
	M2	0.0	7.1	1.2	1.9	6.8	0.8	1.1	11	1.5	3.7	12	5.3	5.4	25	7.9	6.4	41	12	11
	M3	0.0	13	19	17	1.2	11	16	68	65	67	70	38	68	65	14	71	71	69	35
Sku (–)	M1	0.0	0.2	0.1	0.1	0.6	0.7	0.8	1.2	1.6	1.9	1.9	1.9	2.2	2.3	2.2	1.7	0.3	0.7	0.6
	M2	0.0	5.6	2.5	0.7	5.2	2.0	1.4	7.3	2.5	0.1	6.9	2.9	2.3	12	3.4	4.4	22	3.5	13
	M3	0.0	7.5	7.9	7.1	4.8	3.5	2.6	5.5	7.1	10	10	10	7.6	8.7	8.2	13	11	13	8.4
Sp (µm)	M1	0.0	0.4	0.6	0.9	5.8	7.9	8.1	8.2	8.3	8.6	9.1	9.5	10	10	10	11	11	19	21
	M2	0.0	1.2	0.5	0.4	1.1	0.3	0.9	1.1	0.0	0.2	2.4	0.4	0.3	1.9	4.1	7.8	3.6	8.2	11
	M3	0.0	0.7	1.0	0.6	44	45	45	46	46	56	56	57	55	56	56	67	66	66	70
Sv (µm)	M1	0.0	0.5	0.6	1.0	1.1	0.7	0.5	0.4	0.2	0.1	0.6	1.1	1.6	1.6	1.4	4.2	4.1	13	16
	M2	0.0	1.4	0.6	0.5	6.2	7.3	6.6	8.9	7.6	8.9	11	9.3	8.5	24	22	21	28	29	29
	M3	0.0	1.1	1.6	0.9	28	31	30	32	32	32	32	34	38	37	45	47	50	51	64

To get more exact minimum areas the consideration of the standard deviation values can be useful. This can be considered as a modification of the results gained in the first step. In Table 4, the minimum evaluation areas belong to the last standard deviations whose values do not exceed 2% of the basis surface roughness value (measured on the 2 × 2 mm area) are demonstrated.

When comparing the designated minimum areas based on the roughness values and the standard deviation values, it can be observed that the minimum areas are mainly the same. In case of the Sa–M3 pair the surface roughness-based limit is higher (1.3 × 1.3 mm) that the standard deviation-based (1 × 1 mm). In case of the Ssk–M1 pair the standard deviation-based limit (1.7 × 1.7 mm) is higher than the surface roughness-based limit (1.6 × 1.6 mm). The highest areas are considered as minimum evaluation areas. The Ssk and Sku parameters belonging to the M2 and M3 procedure versions resulted in the

maximum area (2 × 2 mm) based on the surface roughness parameter. In these pairs the first calculated standard deviations (for the 1.8 × 1.8 mm areas) exceed the limit, therefore the surface roughness-based limits were considered as relevant. In a study of Yong et al. the measurement area was in the focus. Four evaluation sizes were analyzed from 50 × 50 µm to 5000 × 5000 µm. In case of certain parameters (e.g., Sa, Sq) tendencies were demonstrated in the values but other parameter values showed deviations (e.g., Ssk, Sku) [31].

Table 4. Designated minimum evaluation areas based on the 2% standard deviation limit.

Roughness parameters and machining procedures	**Sa (µm)**	**Sa (µm)**	**Sa (µm)**	**Sq (µm)**	**Sq (µm)**	**Sq (µm)**	**Ssk (–)**	**Ssk (–)**	**Ssk (–)**
	M1	M2	M3	M1	M2	M3	M1	M2	M3
Roughness of the 2 × 2 mm area	0.398	1.127	0.621	0.471	1.378	0.784	0.153	0.666	0.468
2% of the roughness value	0.008	0.023	0.012	0.009	0.028	0.016	0.003	0.013	0.009
Last stdev below the 2% limit	0.003	0.019	0.010	0.000	0.000	0.009	0.002	–	–
Minimum evaluation area (mm × mm)	0.2 × 0.2	0.8 × 0.8	1 × 1	0.2 × 0.2	0.5 × 0.5	1.4 × 1.4	1.7 × 1.7	–	–
Roughness parameters and machining procedures	**Sku (–)**	**Sku (–)**	**Sku (–)**	**Sp (µm)**	**Sp (µm)**	**Sp (µm)**	**Sv (µm)**	**Sv (µm)**	**Sv (µm)**
	M1	M2	M3	M1	M2	M3	M1	M2	M3
Roughness of the 2 × 2 mm area	2.180	2.713	3.279	1.582	3.936	5.862	1.387	3.465	3.598
2% of the roughness value	0.044	0.054	0.066	0.032	0.079	0.117	0.028	0.069	0.072
Last stdev below the 2% limit	0.020	–	–	0.006	0.058	0.024	0.023	0.021	0.027
Minimum evaluation area (mm × mm)	0.2 × 0.2	–	–	1.7 × 1.7	0.6 × 0.6	1.7 × 1.7	0.4 × 0.4	1.7 × 1.7	1.7 × 1.7

3.3. Validation of the Minimum Evaluation Areas

3.3.1. Theoretical Background

Regression analysis is a relatively widely applied tool in 3D roughness analysis. Kumaran et al. stated that the regression model is applicable for analyzing the effect of machining parameters on surface roughness in abrasive waterjet cutting experiments [23]. A similar analysis has been carried out by Kuo et al. in EDM experiments for surface roughness parameter minimization [27].

To analyze the connection between the dependent (roughness parameter) and independent (analyzed surface area) variables (first regression analysis), an estimated linear regression function was determined. The predicted values and the residual values are necessary for the analysis. The predicted values are the values of the regression function in the analyzed points and they are calculated based on the ordinary least square method. The residual values are the differences between the predicted and the measured values. These differences help in determining the variances, i.e., they inform how the data points deviate around the regression line. A residual value is 0 if there is no deviation in the data (line of best fit). In the next step the residual sum of squares (RSS) were calculated in order to eliminate negative values. Then another regression function was determined in order to analyze the effect of the original independent variable to RSS, which measures the level of variance in the residuals (new dependent variable). If the independent variable has no effect on the new dependent variable, the residual value is considered as to be homoscedastic. In this case, the deviation results only from the randomness. The alternative case is the heteroscedasticity of the residual value: the residual value increases with the increase of the independent variable. The value of the significance level was determined according to the Breusch-Pagan test [39]. It informs about the connection between the dependent and independent variables. The hypothesis H0 is considered as fulfilled if the independent variable has no effect on the residual value. This is the homoscedastic case. The meaning of hypothesis H1 is that there is an effect on the residual value (heteroscedasticity). If the significance value (p) is higher than 5%, the hypothesis H0 can be accepted.

3.3.2. Results of the Regression Analysis

Within the minimum evaluation area designated based on the surface roughness and their standard deviation data, the surface roughness shows certain extent of deviation. It has to be proved that the deviation remains low enough with a 95% confidence level. Regression analysis was applied first for the roughness data that remained within the designated limit and then for the residual values.

Regression analyses were carried out for the roughness data points that remain within the limit. If based on the significance level homoscedasticity ($p > 0.05$) resulted for the residuals, the original limit (determined by the highest from the roughness data or the standard deviation) was accepted as the validated minimum evaluation area. In case of heteroscedasticity, further regression analyses were carried out for highest evaluation area limits. This modification was necessary in case of the following surface roughness—machining procedure pairs: Sq–M2 (0.6 × 0.6 mm); Sku–M1 (0.4 × 0.4 mm); Sp–M2 (0.7 × 0.7 mm); Sv–M1 (0.6 × 0.6 mm). In Table 5, the results of the minimization are summarized, and significance levels are given. The regression analysis was applied to modify the minimum evaluation areas determined based on the ±5% limit of the roughness values and the 2% limit of the standard deviation (Section 3.2). The results of this third step can be considered as final results. In Table 5, the minimum areas are underlined.

Table 5. Results of the minimization and the significance levels.

Surface Roughness Parameter	Machining Procedure	Minimum Evaluation Area (mm × mm)			Significance Level (p)
		5% Limit (Surface Roughness)	2% Limit (Standard Deviation)	Regression Analyses	
Sa (µm)	M1	0.2 × 0.2	0.2 × 0.2	0.2 × 0.2	0.823
	M2	0.8 × 0.8	0.8 × 0.8	0.8 × 0.8	0.099
	M3	1.3 × 1.3	1 × 1	1.3 × 1.3	0.512
Sq (µm)	M1	0.2 × 0.2	0.2 × 0.2	0.2 × 0.2	0.089
	M2	0.5 × 0.5	0.5 × 0.5	0.6 × 0.6	0.122
	M3	1.4 × 1.4	1.4 × 1.4	1.4 × 1.4	0.122
Ssk (–)	M1	1.6 × 1.6	1.7 × 1.7	1.7 × 1.7	0.909
	M2	2 × 2	–	2 × 2	–
	M3	2 × 2	–	2 × 2	–
Sku (–)	M1	0.2 × 0.2	0.2 × 0.2	0.4 × 0.4	0.059
	M2	2 × 2	–	2 × 2	–
	M3	2 × 2	–	2 × 2	–
Sp (µm)	M1	1.7 × 1.7	1.7 × 1.7	1.7 × 1.7	0.068
	M2	0.6 × 0.6	0.6 × 0.6	0.7 × 0.7	0.167
	M3	1.7 × 1.7	1.7 × 1.7	1.7 × 1.7	0.401
Sv (µm)	M1	0.4 × 0.4	0.4 × 0.4	0.6 × 0.6	0.576
	M2	1.7 × 1.7	1.7 × 1.7	1.7 × 1.7	0.430
	M3	1.7 × 1.7	1.7 × 1.7	1.7 × 1.7	0.401

4. Conclusions

In this study, a few frequently used 3D height parameters were analyzed with simple descriptive statistical methods and regression analysis. The assumption was that the measured data become more distorted as the size of the evaluated surface area decreases. Hard turned and ground surfaces were analyzed in the study. Minimum evaluation areas

were designated for each analyzed roughness parameter and regression analyses were applied for validating the results.

The main findings of the study:

- There is no clear tendency in the analyzed roughness values when the evaluation area is decreased: the data show oscillation/periodicity (e.g., in the Sa parameter when the surface is hard turned by feed 0.1 mm/rev) in some cases and in others decreasing values (e.g., in the Sq parameter when the surface is machined by infeed grinding) or show irregularities (e.g., in the Sku parameter when the surface is machined by infeed grinding).
- For the Sa, Sq, Sp, and Sv parameters, minimum evaluation areas were determined and validated. Regardless of the machining procedure a 1.3 × 1.3 mm evaluation area can be applied for the Sa parameter, 1.4 × 1.4 mm for Sq, and 1.7 × 1.7 mm for Sp and Sv parameters. These statements are valid only for the analyzed technological data and in the range of surface roughness Sa = 0.4–1.13 μm or Sz = 2.97–9.46 μm.
- Analyzing the Ssk and Sku parameters, valid evaluation areas were determined only in the case of the M1 procedure version (hard turning, f = 0.1 mm/rev). 1.7 × 1.7 mm and 0.4 × 0.4 mm evaluation areas are recommended for the Ssk and the Sku parameters, respectively. In case of the surface hard turned by f = 0.3 mm/rev feed and the ground surface 2 × 2 mm evaluation area is recommended. However, this resulted from the surface roughness and standard deviation limits, and was not validated by the regression analysis.

The novelty of the study is the relatively simple minimization method, which can be expressed to many types of machining procedures. In this paper, it was shown that minimum evaluation areas can be determined. However, generalization of the findings is a necessary further step in surface roughness measurement. Clear designation of evaluation areas could be useful in the industry because the minimization of the area can lead to measurement time savings and therefore lower unit costs, which might be significant in large scale production.

Further research directions based on the results of this study:

- Analysis of other machining procedures (e.g., milling, drilling)
- Analysis of the effects of changes in the technological data based on design of experiment.
- Analysis of more or all roughness parameters.
- Calculation of measurement time savings.

Funding: This research received no external funding.

Institutional Review Board Statement: Not applicable.

Informed Consent Statement: Not applicable.

Data Availability Statement: Not applicable.

Conflicts of Interest: The author declares no conflict of interest.

Appendix A

Examples of studies in 3D surface roughness measurement of surfaces machined by different procedures and the evaluation areas applied.

Table A1. Applied roughness evaluation areas in various cutting technologies.

Cutting Technology	Evaluation Area of 3D Roughness Measurement (mm × mm)
Burnishing	2.5 × 2.5 [40], 3.6 × 3.6 [41]
Direct Laser Deposition	1.2 × 0.9 [42]
Grinding	1.2 × 0.9 [42], 1.5 × 1 [43], 2.5 × 2.5 [16], 0.5 × 0.5 [44]
Hard turning	2.5 × 2.5 [40], 0.5 × 0.5 [44], 0.8 × 0.8 [45]
Honing	1.28 × 1.28 [46]
Milling	1.2 × 0.9 [42], 5 × 5 [47], 2.5 × 2.5 [48], 4 × 4 [49]
Polishing	1.9 × 2.5 [50], 1.75 × 1.75 [51]
Rolling	0.7 × 0.525 [52]
Turning	0.705 × 0.528 [53]

Appendix B

Surface roughness measurement data (area: 2 × 2 mm) and the values generated by the reduction of the area (from 1.9 × 1.9 mm to 0.2 × 0.2 mm) for the three analyzed procedure versions (M1, M2, and M3)

Table A2. Surface roughness values for the procedure version M1.

M1	Side Length of the Measured Area (Square) (mm)									
	2	**1.9**	**1.8**	**1.7**	**1.6**	**1.5**	**1.4**	**1.3**	**1.2**	**1.1**
Sa (µm)	0.398	0.398	0.398	0.397	0.397	0.397	0.398	0.398	0.398	0.398
Sq (µm)	0.471	0.471	0.471	0.470	0.471	0.472	0.472	0.473	0.473	0.473
Ssk (–)	0.153	0.150	0.154	0.151	0.146	0.144	0.139	0.136	0.139	0.132
Sku (–)	2.180	2.184	2.183	2.183	2.193	2.196	2.198	2.207	2.216	2.221
Sp (µm)	1.582	1.575	1.573	1.568	1.491	1.457	1.454	1.452	1.451	1.445
Sv (µm)	1.387	1.394	1.396	1.400	1.403	1.377	1.380	1.382	1.384	1.389
M1	**Side Length of the Measured Area (Square) (mm)**									
	1	**0.9**	**0.8**	**0.7**	**0.6**	**0.5**	**0.4**	**0.3**	**0.2**	
Sa (µm)	0.399	0.400	0.401	0.404	0.405	0.403	0.406	0.403	0.406	
Sq (µm)	0.475	0.476	0.478	0.480	0.482	0.478	0.481	0.477	0.481	
Ssk (–)	0.132	0.125	0.123	0.128	0.128	0.138	0.168	0.146	0.104	
Sku (–)	2.222	2.222	2.228	2.231	2.229	2.218	2.187	2.164	2.194	
Sp (µm)	1.438	1.432	1.426	1.425	1.428	1.411	1.411	1.281	1.247	
Sv (µm)	1.396	1.402	1.409	1.409	1.406	1.329	1.330	1.200	1.170	

Table A3. Surface roughness values for the procedure version M2.

M2	Side Length of the Measured Area (Square) (mm)									
	2	**1.9**	**1.8**	**1.7**	**1.6**	**1.5**	**1.4**	**1.3**	**1.2**	**1.1**
Sa (µm)	1.127	1.102	1.119	1.140	1.105	1.114	1.139	1.102	1.127	1.158
Sq (µm)	1.378	1.354	1.373	1.396	1.356	1.366	1.389	1.355	1.383	1.417
Ssk (–)	0.665	0.713	0.673	0.678	0.710	0.671	0.658	0.736	0.675	0.690
Sku (–)	2.715	2.867	2.784	2.734	2.856	2.770	2.677	2.914	2.782	2.711
Sp (µm)	3.936	3.985	3.957	3.951	3.977	3.925	3.899	3.979	3.935	3.942
Sv (µm)	3.465	3.416	3.444	3.449	3.250	3.211	3.237	3.158	3.201	3.157
M2	**Side Length of the Measured Area (Square) (mm)**									
	1	**0.9**	**0.8**	**0.7**	**0.6**	**0.5**	**0.4**	**0.3**	**0.2**	
Sa (µm)	1.106	1.109	1.150	1.069	1.095	1.159	1.024	1.093	1.240	
Sq (µm)	1.358	1.363	1.402	1.316	1.346	1.406	1.269	1.344	1.475	
Ssk (–)	0.742	0.701	0.701	0.831	0.718	0.708	0.935	0.746	0.741	
Sku (–)	2.902	2.794	2.652	3.042	2.807	2.597	3.324	2.810	2.355	
Sp (µm)	4.030	3.950	3.924	4.012	3.775	3.628	3.792	3.613	3.491	
Sv (µm)	3.070	3.145	3.171	2.639	2.711	2.721	2.480	2.459	2.447	

Table A4. Surface roughness values for the procedure version M3.

M3	Side Length of the Measured Area (Square) (mm)									
	2	**1.9**	**1.8**	**1.7**	**1.6**	**1.5**	**1.4**	**1.3**	**1.2**	**1.1**
Sa (µm)	0.621	0.603	0.608	0.611	0.611	0.615	0.622	0.600	0.589	0.602
Sq (µm)	0.784	0.769	0.776	0.780	0.782	0.788	0.798	0.734	0.747	0.760
Ssk (–)	0.468	0.528	0.557	0.550	0.474	0.415	0.394	0.150	0.164	0.155
Sku (–)	3.279	3.526	3.537	3.513	3.436	3.394	3.363	3.097	3.045	2.949
Sp (µm)	5.862	5.901	5.918	5.896	3.269	3.229	3.221	3.173	3.171	2.598
Sv (µm)	3.598	3.559	3.542	3.565	2.591	2.499	2.507	2.435	2.438	2.431
M3	**Side Length of the Measured Area (Square) (mm)**									
	1	**0.9**	**0.8**	**0.7**	**0.6**	**0.5**	**0.4**	**0.3**	**0.2**	
Sa (µm)	0.605	0.566	0.510	0.510	0.493	0.430	0.428	0.454	0.335	
Sq (µm)	0.766	0.715	0.643	0.641	0.621	0.538	0.534	0.561	0.433	
Ssk (–)	0.139	0.288	0.150	0.163	0.402	0.135	0.135	0.144	0.632	
Sku (–)	2.943	2.966	3.031	2.994	3.010	2.853	2.906	2.848	3.554	
Sp (µm)	2.597	2.542	2.621	2.588	2.580	1.936	1.982	2.010	1.742	
Sv (µm)	2.432	2.382	2.241	2.274	1.993	1.912	1.792	1.764	1.282	

Appendix C

Pictures of the surface topographies after Gauss filtering (scanned area: 2.8 × 2.8 mm; evaluated area: 2 × 2 mm).

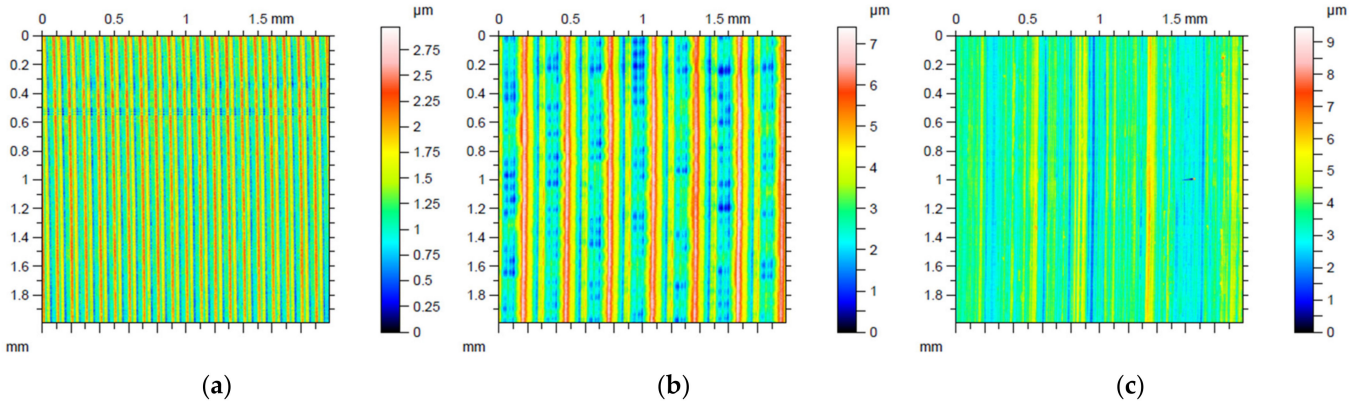

Figure A1. Surface topography of the (**a**) hard turned (f = 0.1) surface—M1 (**b**) hard turned (f = 0.3) surface—M2 (**c**) ground surface—M3.

References

1. Bławucki, S.; Zaleski, K. The effect of the aluminium alloy surface roughness on the restitution coefficient. *Adv. Sci. Technol. Res. J.* **2015**, *9*, 66–71. [CrossRef]
2. Gogolin, A.; Wasilewski, M.; Ligus, G.; Wojciechowski, S.; Gapinski, B.; Krolczyk, J.; Zajac, D.; Krolczyk, G. Influence of geometry and surface morphology of the U-tube on the fluid flow in the range of various velocities. *Measurement* **2020**, *164*, 108094. [CrossRef]
3. Felho, C.; Kundrák, J. Characterization of Topography of Cut Surface Based on Theoretical Roughness Indexes. *Key Eng. Mater.* **2012**, *496*, 194–199. [CrossRef]
4. Sztankovics, I.; Kundrák, J. Theoretical Value of Total Height of Profile in Rotational Turning. *Appl. Mech. Mater.* **2013**, *309*, 154–161. [CrossRef]
5. Kundrak, J.; Felho, C. 3D Roughness Parameters of Surfaces Face Milled by Special Tools. *Manuf. Technol.* **2016**, *16*, 532–538. [CrossRef]
6. Mamalis, A.G.; Kundrak, J. Horvath M: On a novel tool life relation for precision cutting tools. *J. Manuf. Sci. Eng.* **2005**, *127*, 328–332. [CrossRef]
7. Karkalos, N.E.; Karmiris-Obratanski, P.; Kurpiel, S.; Zagorski, K.; Markopoulos, A.P. Investigation on the surface quality obtained during trochoidal milling of 6082 aluminum alloy. *Machines* **2021**, *9*, 75. [CrossRef]

8. Sagbas, A. Analysis and optimization of surface roughness in the ball burnishing process using response surface methodology and desirabilty function. *Adv. Eng. Softw.* **2011**, *42*, 992–998. [CrossRef]
9. Przestacki, D.; Majchrowski, R.; Marciniak-Podsadna, L. Experimental research of surface roughness and surface texture after laser cladding. *Appl. Surf. Sci.* **2016**, *388*, 420–423. [CrossRef]
10. Kumar, R.; Seetharamu, S.; Kamaraj, M. Quantitative evaluation of 3D surface roughness parameters during cavitation exposure of 16Cr–5Ni hydro turbine steel. *Wear* **2014**, *320*, 16–24. [CrossRef]
11. Aidibe, A.; Nejad, M.K.; Tahan, A.; Jahazi, M.; Cloutier, S.G. A Proposition for New Quality 3D Indexes to Measure Surface Roughness. *Procedia CIRP* **2016**, *46*, 327–330. [CrossRef]
12. Linins, O.; Krizbergs, J.; Boiko, I. Surface texture metrology gives a better understanding of the surface in its functional state. *Key Eng. Mater* **2013**, *527*, 167–172. [CrossRef]
13. Khellaf, A.; Aouici, H.; Smaiah, S.; Boutabba, S.; Yallese, M.A.; Elbah, M. Comparative assessment of two ceramic cutting tools on surface roughness in hard turning of AISI H11 steel: Including 2D and 3D surface topography. *Int. J. Adv. Manuf. Technol.* **2016**, *89*, 333–354. [CrossRef]
14. Elbah, M.; Laouici, H.; Benlahmidi, S.; Nouioua, M.; Yallese, M. Comparative assessment of machining environments (dry, wet and MQL) in hard turning of AISI 4140 steel with CC6050 tools. *Int. J. Adv. Manuf. Technol.* **2019**, *105*, 2581–2597. [CrossRef]
15. Li, S.; Chen, T.; Qiu, C.; Wang, D.; Liu, X. Experimental investigation of high-speed hard turning by PCBN tooling with strengthened edge. *Int. J. Adv. Manuf. Technol.* **2017**, *92*, 3785–3793. [CrossRef]
16. Legutko, S.; Zak, K.; Kudlaček, J. Characteristics of geometric structure of the surface after grinding. *MATEC Web Conf.* **2017**, *94*, 2007. [CrossRef]
17. John, J.G.; Arunachalam, N. Illumination Compensated images for surface roughness evaluation using machine vision in grinding process. *Procedia Manuf.* **2019**, *34*, 969–977. [CrossRef]
18. Zhu, L.; Guan, Y.; Wang, Y.; Xie, Z.; Lin, J.; Zhai, J. Influence of process parameters of ultrasonic shot peening on surface roughness and hydrophilicity of pure titanium. *Surf. Coat. Technol.* **2017**, *317*, 38–53. [CrossRef]
19. Mesicek, J.; Ma, Q.-P.; Hajnys, J.; Zelinka, J.; Pagac, M.; Petru, J.; Mizera, O. Abrasive Surface Finishing on SLM 316L Parts Fabricated with Recycled Powder. *Appl. Sci.* **2021**, *11*, 2869. [CrossRef]
20. Zhao, T.; Zhou, J.M.; Bushlya, V.; Ståhl, J.E. Effect of cutting edge radius on surface roughness and tool wear in hard turning of AISI 52100 steel. *Int. J. Adv. Manuf. Technol.* **2017**, *91*, 3611–3618. [CrossRef]
21. Gao, H.; Ma, B.; Singh, R.P.; Yang, H. Areal Surface Roughness of AZ31B Magnesium Alloy Processed by Dry Face Turning: An Experimental Framework Combined with Regression Analysis. *Materials* **2020**, *13*, 2303. [CrossRef] [PubMed]
22. Schwartzentruber, J.; Spelt, J.; Papini, M. Prediction of surface roughness in abrasive waterjet trimming of fiber reinforced polymer composites. *Int. J. Mach. Tools Manuf.* **2017**, *122*, 1–17. [CrossRef]
23. Kumaran, S.T.; Ko, T.J.; Uthayakumar, M.; Islam, M. Prediction of surface roughness in abrasive water jet machining of CFRP composites using regression analysis. *J. Alloys Compd.* **2017**, *724*, 1037–1045. [CrossRef]
24. He, C.; Zong, W.; Sun, T. Origins for the size effect of surface roughness in diamond turning. *Int. J. Mach. Tools Manuf.* **2016**, *106*, 22–42. [CrossRef]
25. Lu, X.; Hu, X.; Jia, Z.; Liu, M.; Gao, S.; Qu, C.; Liang, S.Y. Model for the prediction of 3D surface topography and surface roughness in micro-milling Inconel 718. *Int. J. Adv. Manuf. Technol.* **2017**, *94*, 2043–2056. [CrossRef]
26. Charles, A.; Elkaseer, A.; Thijs, L.; Hagenmeyer, V.; Scholz, S. Effect of process parameters on the generated surface rough-ness of down-facing surfaces in selective laser melting. *Appl. Sci.* **2019**, *9*, 1256. [CrossRef]
27. Kuo, C.; Nien, Y.; Chiang, A.; Hirata, A. Surface modification using assisting electrodes in wire electrical discharge machining for silicon wafer preparation. *Materials* **2021**, *14*, 1355. [CrossRef]
28. Pan, C.; Li, Q.; Hu, K.; Jiao, Y.; Song, Y. Study on Surface Roughness of Gcr15 Machined by Micro-Texture PCBN Tools. *Machines* **2018**, *6*, 42. [CrossRef]
29. Deja, M.; Markopoulos, A. Advances and Trends in Non-Conventional, Abrasive and Precision Machining. *Machines* **2021**, *9*, 37. [CrossRef]
30. Tapoglou, N. Development of Cutting Force Model and Process Maps for Power Skiving Using CAD-Based Modelling. *Machines* **2021**, *9*, 95. [CrossRef]
31. Yong, Q.; Chang, J.; Liu, Q.; Jiang, F.; Wei, D.; Li, H. Matt polyurethane coating: Correlation of surface roughness on measurement length and gloss. *Polymers* **2020**, *12*, 326. [CrossRef] [PubMed]
32. Zawada-Tomkiewicz, A. Analysis of surface roughness parameters achieved by hard turning with the use of PCBN tools. *Estonian J. Eng.* **2011**, *17*, 88. [CrossRef]
33. Pyka, G.; Kerckhofs, G.; Papantoniou, I.; Speirs, M.; Schrooten, J.; Wevers, M. Surface roughness and morphology customization of additive manufactured open porous Ti6Al4V structures. *Materials* **2013**, *6*, 4737–4757. [CrossRef]
34. Pytlak, B. The roughness parameters 2D and 3D and some characteristics of the machined surface topography after hard turning and grinding of hardened 18CrMo4 steel. *Kom. Budowy Masz. Pan–Oddz. W Pozn.* **2011**, *31*, 53–62.
35. Sun, Y.; Jin, L.; Gong, Y.; Qi, Y.; Zhang, H.; Su, Z.; Sun, K. Experimental Investigation on Machinability of Aluminum Alloy during Dry Micro Cutting Process Using Helical Micro End Mills with Micro Textures. *Materials* **2020**, *13*, 4664. [CrossRef] [PubMed]
36. Abouelatta, O.B. 3D Surface roughness measurement using a light sectioning vision system. In Proceedings of the World Con-gress on Engineering, London, UK, 30 June–2 July 2010; Volume 1.

37. Shivanna, D.; Kiran, M.; Kavitha, S. Evaluation of 3D Surface Roughness Parameters of EDM Components Using Vision System. *Procedia Mater. Sci.* **2014**, *5*, 2132–2141. [CrossRef]
38. Kluz, R.; Antosz, K.; Trzepieciński, T.; Bucior, M. Modelling the Influence of Slide Burnishing Parameters on the Surface Roughness of Shafts Made of 42CrMo4 Heat-Treatable Steel. *Materials* **2021**, *14*, 1175. [CrossRef] [PubMed]
39. Zaman, A. *Statistical Foundations for Econometric Techniques*; Academic Press: New York, NY, USA, 1996.
40. Grzesik, W.; Rech, J.; Żak, K. High-precision Finishing Hard Steel Surfaces Using Cutting, Abrasive and Burnishing Operations. *Procedia Manuf.* **2015**, *1*, 619–627. [CrossRef]
41. Dzierwa, A.; Markopoulos, A.P. Influence of Ball-Burnishing Process on Surface Topography Parameters and Tribological Properties of Hardened Steel. *Machines* **2019**, *7*, 11. [CrossRef]
42. Wojciechowski, S.; Twardowski, P.; Chwalczuk, T. Surface roughness analysis after machining of direct laser deposited tungsten carbide. *J. Phys. Conf. Ser.* **2014**, *483*, 012018. [CrossRef]
43. Schmahling, J.; Hamprecht, F.A.; Hoffmann, D.M.P. A three-dimensional measure of surface roughness based on mathematical morphology. In *Technical Report from Multidimensional Image Processing, IWR*; University of Heidelberg: Heidelberg, Germany, 2006.
44. Grzesik, W.; Żak, K.; Kiszka, P. Comparison of Surface Textures Generated in Hard Turning and Grinding Operations. *Procedia CIRP* **2014**, *13*, 84–89. [CrossRef]
45. Matras, A.; Zębala, W.; Machno, M. Research and Method of Roughness Prediction of a Curvilinear Surface after Titanium Alloy Turning. *Materials* **2019**, *12*, 502. [CrossRef] [PubMed]
46. Karolczak, P.; Kowalski, M.; Wiśniewska, M. Analysis of the Possibility of Using Wavelet Transform to Assess the Condition of the Surface Layer of Elements with Flat-Top Structures. *Machines* **2020**, *8*, 65. [CrossRef]
47. Nadolny, K.; Kaplonek, W. Analysis of flatness deviations for austenitic stainless-steel workpieces after efficient surface machining. *Meas. Sci. Rev.* **2014**, *14*, 204. [CrossRef]
48. Kundrak, J.; Nagy, A.; Markopoulos, A.P.; Karkalos, N.E. Investigation of surface roughness on face milled parts with round insert in planes parallel to the feed at various cutting speeds. *Cut. Tools Technol. Syst.* **2019**, 87–96. [CrossRef]
49. Chuchala, D.; Dobrzynski, M.; Pimenov, D.; Orlowski, K.; Krolczyk, G.; Giasin, K. Surface Roughness Evaluation in Thin EN AW-6086-T6 Alloy Plates after Face Milling Process with Different Strategies. *Materials* **2021**, *14*, 3036. [CrossRef] [PubMed]
50. Zhou, H.; Zhou, H.; Zhao, Z.; Li, K.; Yin, J. Numerical Simulation and Verification of Laser-Polishing Free Surface of S136D Die Steel. *Metals* **2021**, *11*, 400. [CrossRef]
51. Zhou, J.; Han, X.; Li, H.; Liu, S.; Shen, S.; Zhou, X.; Zhang, D. In-Situ Laser Polishing Additive Manufactured AlSi10Mg: Effect of Laser Polishing Strategy on Surface Morphology, Roughness and Microhardness. *Materials* **2021**, *14*, 393. [CrossRef]
52. Deltombe, R.; Kubiak, K.J.; Bigerelle, M. How to select the most relevant 3D roughness parameters of a surface? *Scanning* **2014**, *36*, 150–160. [CrossRef]
53. Struzikiewicz, G.; Sioma, A. Evaluation of Surface Roughness and Defect Formation after The Machining of Sintered Aluminum Alloy AlSi10Mg. *Materials* **2020**, *13*, 1662. [CrossRef]